

INTERNAL MOTIONS IN H II REGIONS. XIV. THE BRIGHT RIMMED REGION S135; A BLISTER PHENOMENON?

P. Pişmiş, I. Hasse, and M.A. Moreno

Instituto de Astronomía
Universidad Nacional Autónoma de México

Received 1986 July 3

RESUMEN

Se determinan velocidades radiales por el método de interferometría Fabry-Pérot en 385 puntos dentro y alrededor de la región H II, S135. Esta región muestra un frente ondulante de ionización el cual es más marcado en [N II] $\lambda 6584$ y [S II] $\lambda 6717$ en comparación con $H\alpha$, debido probablemente a un fenómeno de choque. La disminución de la densidad estelar enfrente del borde de ionización indica que una nube oscura está asociada con S135.

Una búsqueda de CO ha descubierto nuevas fuentes a lo largo de la región H II y en la nube oscura con velocidad promedio de -20 km s^{-1} , comparable con la de S135. Dentro y cerca del frente de ionización las velocidades ópticas muestran acercamiento con una velocidad $\cong 4 \text{ km s}^{-1}$ con respecto al conjunto de la nebulosa. Se arguye que el modelo "blister" es consistente con nuestras observaciones.

ABSTRACT

Interferometric FP radial velocities are obtained at 385 points in and around the H II region S135. This region has a very marked undulating ionization front, more intense in [N II] $\lambda 6584$ and [S II] $\lambda 6717$ than in $H\alpha$ due probably to shock phenomena. A paucity of stars in front of the ionized border is indicative of a dark cloud associated with S135. Search for CO in the region has yielded new sources along the H II region and into the dark cloud with an average $V_{\text{LSR}} = -20 \text{ km s}^{-1}$ comparable to the overall optical velocity of S135. At and near the ionization front our optical velocities are by $\cong 4 \text{ km s}^{-1}$ blue shifted with respect to the overall nebula. It is argued that a blister model is consistent with our observations of S135.

Key words: INTERFEROMETRY-FABRY PEROT – H II REGIONS – RADIAL VELOCITIES- $H\alpha$, CO – BLISTER MODEL

I. INTRODUCTION

S135 is a small H II region ($22^{\text{h}}20^{\text{m}}24^{\text{s}}$; $+58^{\circ}29'00''$, 1950.0) with dimensions of 22×15 arcmin (Lynds 1965). It has a very pronounced ionization front along its northwestern edge which is characterized by an undulating outline. The ionizing source is believed to be an O9.5V star at $\alpha = 22^{\text{h}}20^{\text{m}}42^{\text{s}}$, $\delta = +58^{\circ}28'$ (1950) with $V = 9.5$ (Georgelin, Georgelin and Roux 1973). On the Palomar Sky Survey red prints there is a slight paucity of stars past the northwestern boundary of the H II region suggesting the existence of a dark cloud. The systemic radial velocity of S135 is determined using Fabry-Pérot interferometry by Georgelin and Georgelin (1976) and Georgelin *et al.* (1973) but no detailed velocity distribution is given in those papers.

In the radio range, Felli and Churchwell (1972) have included S135 in a continuum 1400 MHz survey of H II regions using the NRAO 300 foot telescope and find a source with flux density of 6.8 fu; despite their low spatial resolution (10 arcmin) this source could be identified with the optical H II region. Blair, Peters and Vanden Bout (1975) study the physical parameters in a

survey of H II regions in CO using the 5-m antenna of the Millimeter Wave Observatory (MWO) of Texas.

Israel (1977) has carried out a "quick look" aperture synthesis survey at $\lambda 6$ and $\lambda 21$ -cm with the Westerbork Synthesis Radio Telescope of several galactic H II including S135; he gives estimates of some physical parameters such as mass ($0.6 M_{\odot}$) and distance (1.9 kpc). In a later paper Israel (1978) presents a statistical study of velocities of H II regions both in CO and in the optical range. Most of the CO data are determined by Israel himself at the WSRT and the MWO telescopes; he discusses the data in terms of the Blister Model. Blitz, Fich and Stark (1982) list this object in a catalogue of CO velocities in the direction of H II regions.

In this paper we present the radial velocity field of S135 obtained through photographic Fabry-Pérot interferometry at 385 points and by the CO molecular line at a few representative points. In Section II we present the observational material; in Section III the morphology of the region. In Section IV we present the optical and CO velocities. In Section V we discuss our results and confront them with those of S140, an H II region similar, in morphology, to S135. Conclusions are given in Section VI.

TABLE 1
OBSERVATIONAL DATA

Plates	α (1950)	δ	Etalon Used ^a (or Direct)	Velocities V_{LSR} (km s ⁻¹)	Number of points	Tele- scope (cm)	Exposure time (Minutes)	Filter ^b used	Date of Observation
FI 375	22 ^h 21 ^m 5	+ 58° 30'	190 Interf.	- 18.05 ± 5.2	83	83	30	H α	Sep. 18, 1977
FI 670	22 21 0	+ 58 38	283 Interf.	- 19.45 ± 4.9	40	83	20	H α	Jul. 13, 1979
FI 675	22 21 0	+ 58 38	283 Interf.	- 19.36 ± 4.5	104	83	55	H α	Jul 14, 1979
FI 809	22 21 5	+ 59 37.9	190 Interf.	- 17.98 ± 7.8	158	212	30	H α	Aug. 30, 1981
FI 811	22 21 45	+ 58 37.8	Direct	212	15	[N II]	Aug. 30, 1981
FI 828	22 21 46	+ 58 37.9	Direct	212	30	[S II]	Oct. 25, 1981
FI 926	22 21 55	+ 58 38.6	Direct	212	10	H α	Sep. 22, 1982

a. The number refers to the free spectral range in km s⁻¹.

b. H α λ 6563 A, [N II] λ 6584 A, [S II] λ 6717 A.

II. THE OBSERVATIONS

All our optical data consisting of Fabry-Pérot interferograms as well as of direct images were obtained with a focal reducer mounted at the Cassegrain focus of either the 83-cm or 2.1-m reflectors of the Observatorio Astronómico Nacional at San Pedro Mártir, Baja California. We have used, throughout, a one-stage Varo image intensifier and Kodak 103aG films. The scale on the photographs is 120 arcsec with the 83-cm and 49 arcsec with the 2.1-m telescopes. The interferograms were taken in the H α line through a 10A (FWHM) interference filter centered at λ 6563A. Two different FP étalons were used as specified in Table 1. The interferograms were measured for radial velocity on photographic enlargements. Test for the reliability of this procedure carried out earlier by comparison with measurements on a Mann comparator used in our previous papers of the series have yielded positive results. The list of interferograms and direct images is given in Table 1. The velocity points were compared with the direct images in H α and all points affected by convolution were left out. Table 1 also lists the average LSR velocities from each interferogram.

The first column gives the identification of the plate, the second and third, the coordinates. The fourth column gives the étalon used (if not a direct plate) and the fifth, the average LSR velocity with standard deviations, followed by the number of points (6), the telescope used (7) and the exposure time (8). The two last columns give the filter used (9) and the date of observation (10).

The largest differences in the average velocities between interferograms do not exceed 1.5 km s⁻¹; given the natural dispersion of the velocities in HII regions and the fact that the interferograms do not overlap completely, the difference in the averages is quite acceptable.

III. MORPHOLOGY

Figures 1,2 and 3 (Plates) are the images of S135 in the line radiation of H α , [N II] λ 6584 and [S II] λ 6717

respectively, as specified in Table 1. A very pronounced undulating ionization front at the north-west dominates the morphology of S135. That front is more contrasted in [N II] and [S II] implying that shock phenomena are operative in that zone. In Figure 4 (Plate) we show a reproduction of this HII region from a POSS red print. Beyond the ionization front a paucity of stars is clearly seen extending towards the north, a strong indication that a dark cloud is associated with S135. CO observations to be commented upon later indicate that this HII region is indeed closely related to a molecular cloud.

The undulating form of the rim is probably caused by density inhomogeneities in the molecular cloud. The direct images in [N II] and [S II] (Figures 2 and 3) exhibit enhanced arcs and ridges within the HII image due presumably to such inhomogeneities.

S135 resembles the HII region S140 in that the latter is also at the border of a CO dark cloud, Lynds 1204, which is much more extended on POSS red plates as compared to the dark cloud of S135. This is clearly seen in Figure 5 (Plate), a reproduction of S140 from POSS red prints.

IV. VELOCITY FIELD

We have deemed it unnecessary to present the velocity field with all 385 measured velocity points. Instead the region is divided into subregions sketched in Figure 6, following roughly the morphology of S135 based on a direct H α image. (Such division evidently tends to be subjective). In that figure the velocity averages over each subregion is inscribed together with their standard deviations and the number of points used.

The average optical velocities in the subregions show a rather wide range of values. The outlying faint patches yield an overall LSR velocity which is less in absolute value as compared to the HII region proper.

The overall average LSR velocity is -18.5 km s⁻¹. However, the general trend noted is that the brightest parts which we consider HII region proper tend

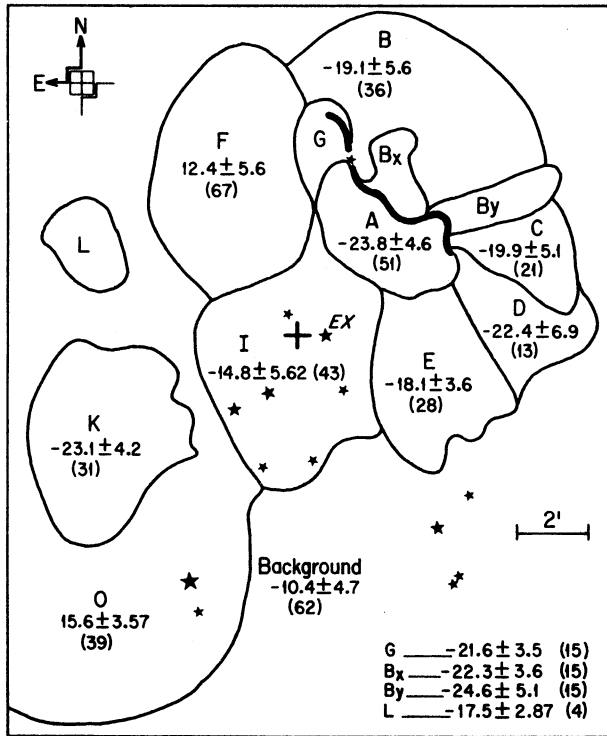


Fig. 6. Subregions into which the area around S135 is divided following roughly the morphology of the H α emission based on a photograph taken with the 83-cm reflector of the Observatory at San Pedro Mártir, México. The average velocity within each subregion is given, together with its standard deviation and the number of points used. The cross marks the position (α, δ) of Israel's (1978) CO observations. The star marked EX is believed to be the ionization source. The curved line represents the bright rim of S135.

to be 3-4 km s⁻¹ blue shifted with respect to their immediate surroundings. Thus the outlying faint patches are in general more red shifted than the HII region proper.

Blair, Peters and Vanden Bout (1975) have determined ¹²C¹⁶O line intensities using the 5-m telescope of the MWO at two points with antenna temperatures of 16 and 17 K and LSR velocities of -17, -16.5 km s⁻¹ respectively. Israel has observed in the same transition line of CO also two points with antenna temperatures of 3.4 and 8.0 K and LSR velocities of -20.8 and -20.8 km s⁻¹ respectively.

The optical resemblance between S135 and S140 (associated with a molecular cloud where CO sources have been detected) prompted us to look into the ¹²C¹⁶O radiation across the ionization front of S135 and into the dark cloud. To that end a direction was selected with PA = -45° passing through the point marked 0,0 by Israel (1978) with coordinates = 22^h20^m18^s = +58° 28' (1950).

Our CO observations are due to L.F. Rodríguez who carried them out at the 12-m telescope of NRAO¹ at Kitt Peak. The size of the beam was 30 arcsec, $\lambda = 1.3$ mm and $\Delta V = 0.33$ km s⁻¹. Table 2 lists the observational details and the velocities obtained. Of the eleven points observed only at seven, nearest the central one (0,0 of Israel's), was CO detected. The spatial limit up to which CO was observable coincides, by eye estimate, with the boundary of the paucity of stars (Figure 4—Plate) hence that of the dark cloud. There is a slight variation in the

1. The National Radio Astronomy Observatory is operated by Associated Universities, Inc., under contract with the National Science Foundation.

TABLE 2^a

¹²C¹⁶O AND H α VELOCITIES OF S 135

Position		Radial Velocities ¹² C ¹⁶ O		Average V _{LSR} H α	Number of points
α (1950)	δ	V _{LSR} (km s ⁻¹)	°K		
22 ^h	20.3 ^m	+ 58° 28'	- 20.5	0.893	
22	20.16	+ 58 29	- 19.5	1.158	21
22	20.03	+ 58 30	- 18.9	12.667	
22	19.9	+ 58 31	- 19.5	11.567	44
22	19.76	+ 58 32	- 20.2	10.433	
22	19.63	+ 58 33	- 20.5	2.340	18
22	19.5	+ 58 34	- 20.5	1.187	
22	19.36	+ 58 35	
22	19.23	+ 58 36	
22	19.1	+ 58 37	
22	18.96	+ 58 38	

a. See Figure 7. At the four last points, on the west side, marked on the map, no CO was detected within the limits of sensitivity.

velocity along the PA -45° line, the outer three points being by $\sim 1.1 \text{ km s}^{-1}$ more negative. We mention this in passing only, without attaching any physical significance, and take the average LSR velocity of -20 km s^{-1} to represent the systemic velocity of the CO cloud. In Figure 7, we present our CO observations to be discussed below together with some optical velocity averages. In that figure Blair *et al.*'s points are marked by open circles and Israel's points, by filled circles.

For a comparison of the optical velocities with those of CO we have proceeded as follows: In Figure 7 we have drawn circles equal to the beam size along six points where CO was observed. The number within each circle is the measured CO velocity. At the last four points no CO was detected. We have also drawn large circles with centers on the 45° line as indicated in Figure 7. The numbers inscribed are the averaged out values of the optical velocities that fall within each circle together with the number of velocity points and standard deviations.

The $H\alpha$ velocities starting from the neighborhood of the ionizing star towards the bright rim clearly show a blue shift indicating that ionized gas is flowing away from the CO cloud towards the observer with a line of sight component of $\cong 4 \text{ km s}^{-1}$ with respect to the immediate background $H\alpha$ emission and to the CO velocities of -20 km s^{-1} . Our CO velocities are quite comparable to Israel's but Blair *et al.*'s values are systematically more positive.

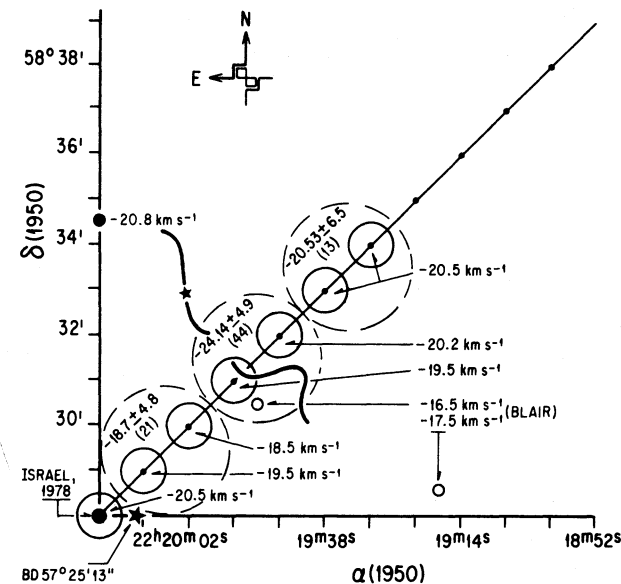


Fig. 7. Presents our CO observations and some averages of $H\alpha$ velocities. Within the large circles marked with broken lines are given the average $H\alpha$ velocities determined by Fabry-Pérot interferometry. Open circles indicate Blair *et al.* (1975)'s CO observations while filled circles, those of Israel (1978). The bright rim is marked by a thick undulating line. Small circles are equal to the beam size. The 11 points where CO was searched are indicated along the PA -45° line. The LSR velocities at 7 of these points are also marked. No CO was detected at the 4 outer points within the sensitivity limit.

V. DISCUSSION

In Section III we had called attention to the morphological resemblance of S135 to S140 studied by us earlier (Pişmiş, Moreno and Hasse 1979). We now compare the kinematics of these two regions. The mean velocity (from Fabry-Pérot interferometry) of the HII region S140 is $V_{\text{LSR}} = -9.2 \text{ km s}^{-1}$ (183 points) while the CO velocities yield $V_{\text{LSR}} = -8.0 \text{ km s}^{-1}$. The blue shift of the emission lines, 1.2 km s^{-1} , however is very small. S140 has the peculiarity that on both sides of the ionization front the velocities V_{LSR} are redshifted with respect to the overall nebula, by 1 km s^{-1} hence they are very slightly more positive than the rest of the HII region (Pişmiş *et al.* 1979). The consistency of the velocity field of S140 with that of a simple blister model appears thus to be marginal. However, this may also be due to a projection effect.

Our kinematic distance of S135 based on a systemic LSR velocity of -18.5 km s^{-1} is 1.9 kpc using the Schmidt rotation law. Georgelin *et al.* give 1.88 kpc while Israel adopts 1.9 kpc for the same object; thus all three values are comparable. S140 on the other hand has a kinematic distance of 0.9 kpc by Pişmiş *et al.* (1979) and 1.06 by Georgelin *et al.* (1973), both estimates based again on the Schmidt rotation curve. The ratio of the distances of S135 to S140 is therefore nearly 2. As regards their projected dimensions, S140 is about 30 arcmin along its bright rim while S135 is about 15 arcmin. The projected linear dimensions of the bright rims of both S135 and S140, would therefore be about 8 parsecs. Hence the curious coincidence that S135 and S140 have comparable linear sizes at their ionization front! We also note that the projected distance of the ionizing star of S140 from the ionization front is, again, twice that for S135.

No line splitting is detected in any of our interference patterns; only a relative velocity of approach is shown by our data. The velocity of approach of the brighter parts of S135 might be due to the circumstance that the region (if we assume it expanding) is located at the nearer edge of a dark cloud such that we are observing only the approaching side of the nebula, the back side, the presumably red shifted part, being unobservable due to extinction. However, this interpretation does not seem likely. If the line of sight dimension is comparable to the projected one the thickness would be around 8 parsecs; at that depth extinction might not be high enough to block the receding edge.

A more likely explanation of the observations can be had by invoking the so-called "Blister Model". The model was proposed originally by Zuckerman (1973) to explain the anomalous motions of ionized gas in the Orion nebula. The argument is that ionized gas is streaming away from the ionization front as a result of the interaction of the HII region with the coexisting molecular cloud. Other workers, rather independently of one another (Balick 1974; Dopita, Dyson and Meaburn

1974), have proposed much the same mechanism of interaction at sites where dark clouds coexist with H II regions.

In a statistical study of the structure of H II regions Israel (1978) finds evidence of the blister phenomenon. Based on optical and CO velocities he shows that the difference in the velocity $\Delta V = V(\text{H II}) - V(\text{CO})$ of 51 visible (unobscured) H II regions is negative ($\Delta V = -3.4 \pm 0.4 \text{ km s}^{-1}$) confirming thus "an essential property of the blister model, namely that ionized gas is flowing away from the dark CO cloud associated with the H II region". The distribution of the obscured H II regions does not show a blue shift; this result does not seem to contradict the blister model (Israel 1978). In any case the observed relative blue shifts are rather small rarely exceeding 4 km s^{-1} .

The $\text{H}\alpha$ velocities of S135 proper, reported here, are blue shifted with respect to those of the CO by $3\text{-}4 \text{ km s}^{-1}$ (3.2 km s^{-1} on average, see Figure 7), hence S135 is one of those cases where the H II region is at the near side of the CO cloud; thus it appears that a blister model is applicable to our observations.

It may be interesting to note that a very pronounced blister phenomenon is observed at a bright-rim of the giant H II region IC 1848 (also W5). The rim, W5A, at the eastern border of W5, one of its seven bright rims, has a large CO cloud west of it, in which IR sources are embedded (Wilking *et al.* 1984). Fabry-Pérot LSR velocities of the rim (-52 km s^{-1}) show a blue shifted of $10\text{-}12 \text{ km s}^{-1}$ with respect to the systemic velocity of the giant H II region and of the CO cloud (both around -40 km s^{-1} (Pişmiş and Hasse 1986, in preparation). The difference of 12 km s^{-1} between the bright rim W5A and the CO cloud is perhaps the largest observed so far in the blister model.

VI. CONCLUSIONS

Summarizing, we may state that the H II region S135 with a pronounced ionization front is exhibiting its interaction with the CO cloud with which it is associated. The CO velocities in general do not differ from the systemic LSR velocity of -20 km s^{-1} while our $\text{H}\alpha$ velocities at and near the ionization front show a blue-

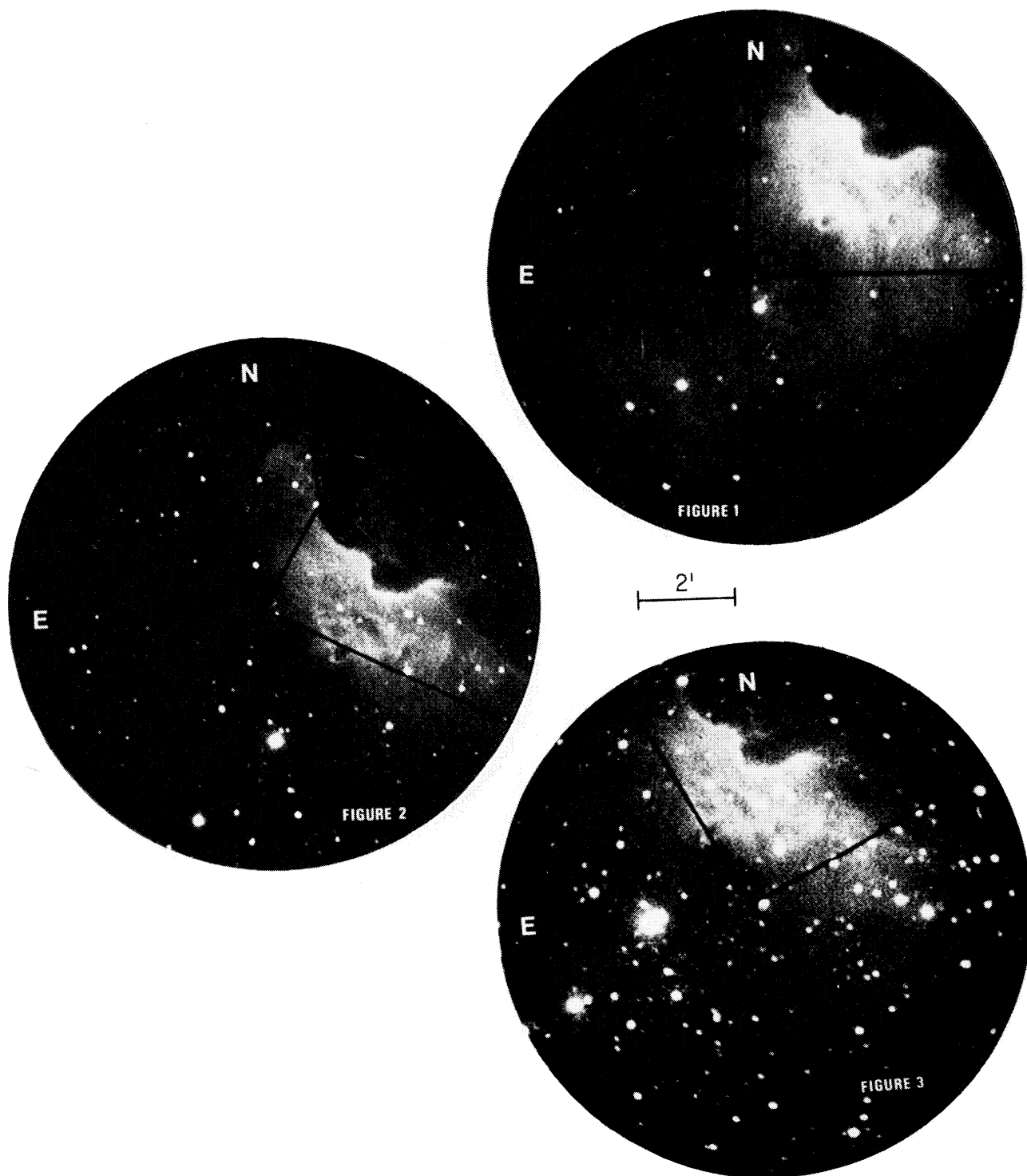
shift, hence a relative approach, an expansion, with respect to the CO velocities. The expansion velocity increases slightly from the location of the ionizing star towards the bright rim and beyond. The resulting average blueshift is at least 3.2 km s^{-1} . Past the ionization front and about 4 arcmin into the dark cloud, going along the direction of our molecular observations, the CO cloud appears to terminate (within the sensitivity attained) roughly where the paucity of stars terminates. We believe therefore that S135 is a specimen of a Blister model with which our observations are consistent. It would be interesting to search for IR sources in the region of S135, particularly in the molecular cloud facing the ionization front.

We are indebted to L.F. Rodríguez who most kindly devoted part of his observing run at the 12-m NRAO telescope to provide us with the CO observations discussed here. His generosity is indeed highly appreciated. We also acknowledge the photographic and drafting work done by L. Quijada and A. García respectively, and help at the telescope by A. Quintero.

REFERENCES

- Balick, B., Gammon, R.M., and Hjellming, R.M. 1974, in *H II Regions and the Galactic Center*, ed. A.F.M. Moorwood, 8th SLAB Symposium, ESRO SP-105, p. 28.
- Blair, G.N., Peters, W.L., and Vanden Bout, P.A. 1975, *Ap. J.*, **200**, L 161-L164.
- Blitz, L., Fich, M., and Stark, A.A. 1982, *Ap. J. Suppl. Series*, **49**, 183.
- Dopita, M.A., Dyson, J.E., and Meaburn, J. 1974, *Ap. and Space Sci.*, **28**, 61.
- Felli, M. and Churchwell, E. 1972, *Astr. and Ap.*, **5**, 369.
- Georgelin, Y.M. and Georgelin, Y.P. 1976, *Astr. and Ap.*, **49**, 57.
- Georgelin, Y.M., Georgelin, Y.P., and Roux, S. 1973, *Astr. and Ap.*, **25**, 337.
- Israel, F.P. 1978, *Astr. and Ap.*, **70**, 769.
- Lynds, B.T. 1965, (*Ap. J. Suppl.*, **12**, 163.
- Pişmiş, P. and Hasse, I. 1986, in preparation.
- Pişmiş, P., Moreno, M., and Hasse, I. 1979, *Rev. Mexicana Astron. Astrof.*, **4**, 331.
- Thronson, Jr., H.A., Thompson, R.I., Harvey, P.M., Rickard, L.J., and Tokunaga, A.T. 1980, *Ap. J.*, **242**, 609.
- Wilking, B.A., Harvey, P.M., Lada, C.J., Joy, M., and Doering, C.R. 1984, *Ap. J.*, **279**, 291.
- Zuckerman, B. 1973, *Ap. J.*, **183**, 863.

INTERNAL MOTIONS IN H II REGIONS



Figs. 1 to 3. Images of S135 in the line radiation of $H\alpha$, $[N II] \lambda 6584$ and $[S II] \lambda 6717$ respectively. These are taken with a focal reducer and a 1-stage image tube attached to the Cassegrain focus of the 2.12-m reflector of the Observatorio Astronómico Nacional at San Pedro Mártir, B.C., México. The filters used have a FWHM of 10Å; 103aG films are used throughout; the scale on the original film is $49 \text{ arcsec mm}^{-1}$. The brightest star on all images is believed to be the ionizing source.

P. Pişmiş *et al.* (See pag. 131)

INTERNAL MOTIONS IN H II REGIONS

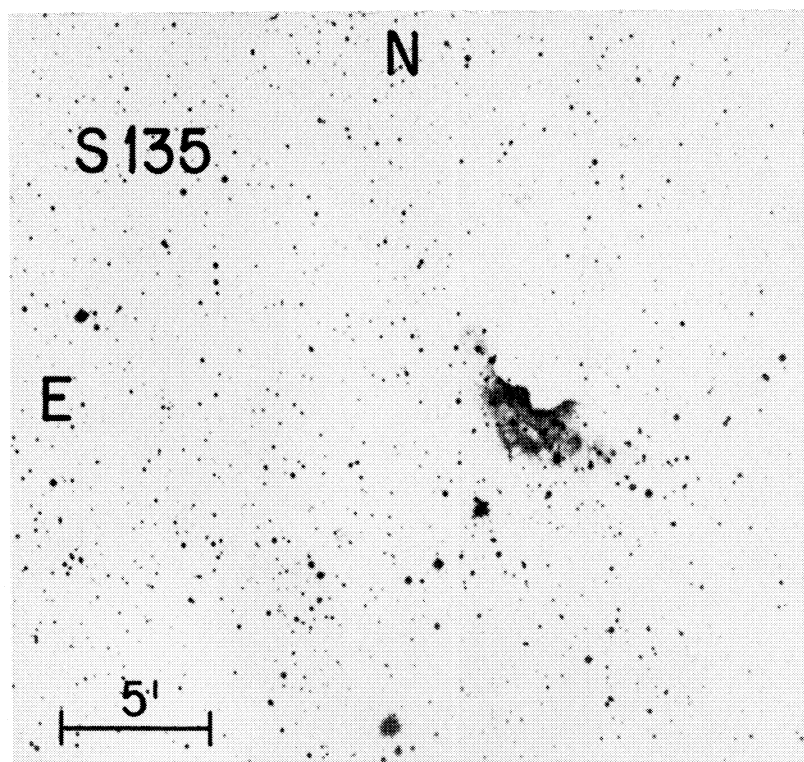


Fig. 4. Region of S135 from a POSS red print.

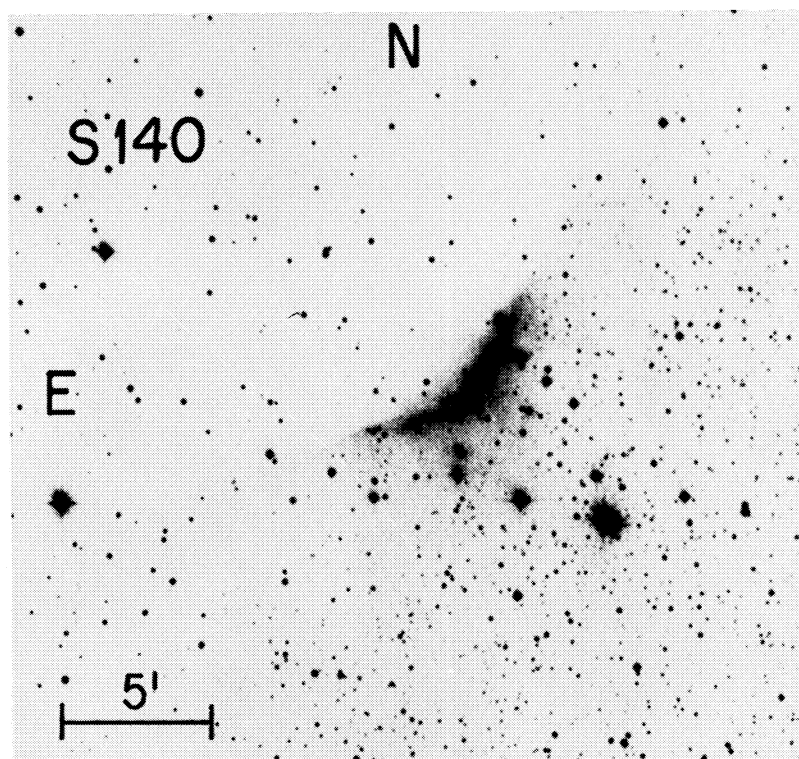


Fig. 5. Region of S140 from a POSS red print.

P. Pişmiş *et al.* (See pag. 131)